Structural Engineering and Mechanics, *Vol. 47, No. 1 (2013) 1-25*
DOI: http://dx.doi.org/10.12989/sem.2013.47.1.001

Modeling of combined thermal and mechanical action in roller compacted concrete dam by three-dimensional finite element method

A.A. Abdulrazeg[*1], J. Noorzaei[2a], T.A. Mohammed[2a] and M.S. Jaafar[2a]

[1]*Civil Engineering Department, Omar Al Mukhtar University, Libya*
[2]*Civil Engineering Department, Universiti Putra Malaysia, UPM-Serdang, Malaysia*

(Received April 6, 2011, Revised April 29, 2013, Accepted June 8, 2013)

Abstract. A combined thermal and mechanical action in roller compacted concrete (RCC) dam analysis is carried out using a three-dimensional finite element method. In this work a numerical procedure for the simulation of construction process and service life of RCC dams is presented. It takes into account the more relevant features of the behavior of concrete such as hydration, ageing and creep. A viscoelastic model, including ageing effects and thermal dependent properties is adopted for the concrete. The different isothermal temperature influence on creep and elastic modulus is taken into account by the maturity concept, and the influence of the change of temperature on creep is considered by introducing a transient thermal creep term. Crack index is used to assess the risk of occurrence of crack either at short or long term. This study demonstrates that, the increase of the elastic modulus has been accelerated due to the high temperature of hydration at the initial stage, and consequently stresses are increased.

Keywords: FEM; roller compacted concrete dam; thermal stress; creep; mechanical behavior; crack criterion factor

1. Introduction

RCC dams are vulnerable to cracking as a result of high tensile stresses due to thermal loads, material properties, and mechanical loads. Making reliable prediction of stresses fields, and thereby cracking risk, thermal and mechanical properties such as creep form an important part of the material modeling. Recently, many models have been proposed to study the significance of thermal loads and creep on RCC dam. For instance, an incremental analysis formulation, modeling the construction sequence, was employed to determine the influence of thermal loads and creep on the structural response during and after construction (Truman 1991). Therefore, performing such an analysis will lead to better prediction of crack propagation (Bombich 1987, Fehl *et al*. 1988, Truman 1991).

Temperature rising in a RCC dam due to hydration of concrete, environmental boundary conditions and quick construction process can induce a high thermal gradient in interior mass and

∗Corresponding author, Lecturer, E-mail: aied@omu.edu.ly
[a]Professor

http://www.techno-press.org/?journal=sem&subpage=8 ISSN: 1225-4568 (Print), 1598-6217 (Online)

exterior surface of the dam (Noorzaei *et al*. 2006). Temperature does not only influence the properties of concrete such as elastic modulus and creep properties, but also induces thermal stresses. The temperature increase, accelerates both the initial elastic modulus and the creep rate of concrete (Wu and Luna 2001). In addition, temperature induces additional creep component (transient thermal creep) which develops at the time of a temperature increase.

Cervera *et al*. (2000a, b) presented a numerical procedure to simulate the construction process of RCC dams. In this work, a thermochemical model was proposed to simulate the hydration and aging processes of concrete and predict the evolution of the thermally induced stresses in concrete at early ages. However, two dimensional model was adopted in this study. In addition, thermal exchange between the reservoir and dam body was ignored. In the same year, (Luna and Wu 2000) used three dimensional finite element modeling to simulate the sequence of construction of Jinagya RCC dam. The effect of temperature on the elastic modulus and the creep behavior of concrete was considered. This work was carried during the construction stages only. However, to simulate the temperature and stress fields completely, both of these fields also need to be simulated during the operation time (after the reservoir is filled with water).

Jaafar *et al*. (2007) dealt with the development of a finite element modeling based computer code for the determination of temperatures within the dam body. The finite element code was then applied to the real full-scale problem to determine the impact of the placement schedule on the thermal response of RCC dam. In the presented study only thermal analysis was preformed.

A distribution of temperature and stress of Xiaowan gravity dam in China was simulated by (Lingfei and Li 2008). Several factors affecting dam temperature and stress such as thermal and mechanical properties, concrete construction, temperature variation of environment were taken into account in the numerical simulation. However, the aging and thermal effects on the elastic properties were ignored. later on, a three- dimensional finite element relocating mesh method developed by Zhang *et al*. (2009) to simulate construction process of RCC dam. In this work, thermal adiabatic rise of temperature with age, the process of placement by layer, creep and the change of air temperature were considered. However, the study was limited for thermal analysis only.

The stress field distribution of RCC dam cannot be achieved satisfactory, because of the complex distribution of the temperature changes throughout the dam body, significant influence of creep on the stress and the significant difference between the mechanical characteristics of the incremental blocks' left (Santurjian and Kolarow 1996). Thus, to reach reliable estimation of the stress field distribution, factors such as concreting dates, corresponding mechanical properties, thermal effect on concrete properties and creep must be considered in the analysis (de Araújo and Awruch 1998, Sheibany and Ghaemian 2006). Besides the mentioned condition a three dimensional analysis is required for thermal stress problem of mass concrete (Ishikawa 1991, Santurjian and Kolarow 1996).

It is evident from the above literature review that, continuous efforts should be made to arrive at realistic numerical modeling of stress fields in RCC dam, in construction and operation phases. There are several research work have been carried out concerning the RCC dams, some of them representing specialized computer programs, reported in the literature (Cervera *et al*. 2000b, Crichton *et al*. 1999, Ishikawa 1991, Malkawi *et al*. 2003). Most of the investigators idealized dam as two dimensional, and the creep is considered very approximately or neglected (Agullo and Aguado 1995, de Araújo and Awruch 1998, Saetta *et al*. 1995). However, due to the significant influence of creep on the stress values, especially in early age concrete (Santurjian and Kolarow 1996) more accurate creep model is essential. Furthermore, consistent cracking criterion is also

necessary for an exact evaluation of the dam behavior. Most of the previous researchers who investigated dam concrete mainly focused on the uniaxial compressive strength and tensile strength, so their studies did not provide information on the behavior of dam concrete under bi-axial or tri-axial stress states (Wang and Song 2008).

2. Motivation of the present work

The present investigation is a continuation of authors' previous work (Abdulrazeg *et al*. 2010) and presenting a numerical implementation using three- dimensional finite element method to simulate the construction process and the first 3 years of service life of RCC dams. The primary objectives of the present research work;

(a) To propose a mathematical visco-elastic model, which account for the ageing and temperature dependent properties of concrete.

(b) To develop a mathematical crack model for RCC materials which include the effect of aging and temporal domain on its formation to establish reliably precise safety evaluation of the RCC dam behavior.

(c) To apply the proposed model to a simple concrete block and an actual RCC dam to demonstrate the efficiency of the model.

3. Computation of thermal field

The numerical solution scheme used in this study is based on the Taylor–Galerkin approach. Upon applying this approach, the following system of differential equations is obtained (Bayagoob *et al*. 2010)

$$[\mathrm{K_t}]^{(e)}\{\mathrm{T}\}^{(e)} - [\mathrm{C}]^{e}\left\{\frac{\partial \mathrm{T}}{\partial \mathrm{t}}\right\}^{(e)} = \{\mathrm{F}\}^{(e)} \tag{1}$$

where, $[C]^e$ is the capacitance matrix; $[C_t]$ is the heat stiffness matrix; $\{F\}$ is the total load heat vector due to hydration and convection actions.

The finite difference approximation was used to solve Eq. (1) in the time domain numerically

$$\left([\mathrm{C}]+\theta\Delta\mathrm{t}[\mathrm{K_t}]\right)\{\mathrm{T}\}_{\mathrm{b}} = \left([\mathrm{C}]+\theta\Delta\mathrm{t}[\mathrm{K_t}]\right)\{\mathrm{T}\}_{\mathrm{a}} + \Delta\mathrm{t}\left((1-\theta)\{\mathrm{F_t}\}_{\mathrm{a}} + \theta\{\mathrm{F_t}\}_{\mathrm{b}}\right) \tag{2}$$

where $\{T\}_b$ and $\{F_t\}_b$ are $\{T\}$ and $\{F_t\}$ at time (b) and $\{T\}_a$ and $\{F_t\}_a$ are $\{T\}$ and $\{F_t\}$ at time (a), θ is a scalar ($0 \le \theta \le 1$) which is equal to 2/3 in the Galerkin method.

4. Viscoelastic behavior of concrete

One of the main characteristics of concrete that distinguishes it from the traditional viscoelastic materials is the time-dependent effect (Yuan and Wan 2002). The Boltzmann's principal of superposition of strains, which first was modified by Neville *et al*. (1983) to include the effect of aging of concrete, states that: the strains produced in concrete at any time t by a (tensile or

compressive) stress increment applied at time τ are independent of the effect of any stress applied either earlier or later than time τ, but does depend on τ (Atrushi 2003). Thus, summing the strain history due to all small stress increments before time t, may write the creep law for uniaxial stress in the form as

$$\varepsilon(t) = \int_{\tau}^{t} J(t,\tau) d\sigma(\tau) + \varepsilon^{0}(t) \tag{3}$$

where t is current time (measured from casting of concrete), τ is concrete age at loading, $d\sigma(\tau)$ is stress increment applied at τ, $\varepsilon(t)$ is total strain, $\varepsilon^{0}(t)$ stress-independent strain and $J(t, \tau)$ is creep compliance.

4.1 Creep compliance

The exponential model of creep has been attractive from the computation point of view, because it can avoid storing the whole stress history and made the implementation feasible comparing with other models (Abdulrazeg *et al*. 2010).

The creep functions may be expressed with Dirichlet series (Wu and Luna 2001) as

$$J(t,\tau) = \sum_{\gamma=1}^{M} \frac{1}{\mu_{\gamma}(\tau)} [1 - e^{y_{\gamma}(\tau) - y_{\lambda}(t)}] \tag{4}$$

where is $J(t,\tau)$ creep functions, $\mu_{\gamma}(\tau)$ is function of one variable, called the reduced times, τ is the loading age in days, $y_{\gamma}(\tau)$ is experimental function. Neglecting temperature effects, a specific form of the compliance function is often used (Du and Liu 1994)

$$J(t,\tau) = C(t,\tau) + \frac{1}{E(\tau)} \tag{5}$$

where $C(t,\tau)$ is creep compliance, it can be expressed as

$$C(t,\tau) = \sum_{\gamma=1}^{3} \varphi_{\gamma}(\tau) [1 - e^{-S_{\gamma}(t-\tau)}] \tag{6}$$

$$\varphi_1 = \alpha_1 + \beta_1 \tau^{-\delta 1}, \quad \varphi_2 = \alpha_2 + \beta_2 \tau^{-\delta 2}, \quad \varphi_3 = De^{-S_3 \tau}$$

where α_{γ}, β_{γ} , δ_{γ}, D, S_{γ} are constants determined from the experimental data.

$E(\tau)$ is elastic modulus, and the model which was developed by (Conrad *et al*. 2003), has been adopted in this study. This model expresses the variation of the elastic modulus of RCC material with time

$$E(\tau) = E_c e^{a\tau^{b}} \tag{7}$$

where E_c is the final elastic modulus, a and b are model parameters.

5. Influence of temperature

Bazant *et al.* (2004) introduced the concept of the degree of hydration to include the temperature influence. Term equivalent age τ_e, which represents the hydration period for which the same degree of hydration is reached at a current temperature as that one reached during the actual time (t) at a reference temperature. The concrete age, τ will be replaced by equivalent age τ_e in the exponential model Eq. (6).

$$\tau_e = \int_0^{\tau} \beta_\tau(t)dt \tag{8}$$

where $\beta(t)$ is a function of current temperature and expressed as

$$\beta_\tau(t) = e^{\Pi_h(\frac{1}{T_r}+\frac{1}{T(t)})} \tag{8a}$$

where $T(t)$ is a current temperature, T_r = 20°C, Π_h is function of hydration degree =2700 K. To consider the temperature effect on the creep compliance, a function $y_\gamma(t)$ is introduced as

$$y_\gamma(t) = S_\gamma \int_0^{t} \psi_T(t)dt \tag{9}$$

where $\psi_\tau(t)$ is a function of current temperature and expressed as

$$\psi_\tau(t) = e^{\Pi_\alpha(\frac{1}{T_r}+\frac{1}{T(t)})} \tag{9a}$$

where Π_α is function of activation energy of creep =5000 K.

Using the introduced term of equivalent age τ_e, which represents the hydration period, the concrete age, τ will be replaced with this equivalent age τ_e in the above elastic modulus Eq. (7). So, the modified model includes both aging and temperature effects (Abdulrazeg *et al*. 2010).

5.1 Creep at variable temperature

For changing temperature conditions while the concrete is under load, an additional creep component, the so-called transient thermal creep, which develops at the time of a temperature increase should be considered (Bosnjak 2000). Transient thermal creep is interdependence between temperature response and mechanical response, and based on that the thermal strain rate should be made dependent on the current stress state (Thelandersson 1987)

$$\Delta\varepsilon_T = \alpha\Delta T\left(1+\xi\frac{\sigma}{f_c}\right) \tag{10}$$

Where $\Delta\varepsilon_T$ is thermal strain increment, σ current stress, $\bar{f}_c$ is uniaxial compressive strength at reference temperature, ΔT is temperature change, ξ model parameter and α coefficient of thermal expansion.

Jonasson (1994) applied Eq. (10) to young concrete and further modified the Eq. (10) and expressed as

$$\Delta\varepsilon_T = \alpha\Delta T\left(1+\xi\frac{\sigma}{f_t}\Delta T\right) \tag{11}$$

Where f_t is the tensile strength at reference temperature and ξ range between (0.1- 0.7) the best value for ξ fitted to the test results was 0.27(Hedlund 1996).

6. Mathematical model of creep

To predict the response of the concrete in the early period of construction, a step-by-step method is necessary. At the beginning of each time step, deformation due to thermal variation (hydration and environment) and creep during the current time interval is imposed. The imposed incremental strain on any point at i^{th} time interval is defined as

$$\Delta\varepsilon_n = \Delta\varepsilon_n^e + \Delta\varepsilon_n^c + \Delta\varepsilon_n^T + \Delta\varepsilon_n^{Trcr} \tag{12}$$

where $\Delta\varepsilon_n^e, \Delta\varepsilon_n^c, \Delta\varepsilon_n^T, \Delta\varepsilon_n^{Trcr}$ refer to elastic, creep, temperature and transient thermal creep strain increment column vectors, respectively.

Wu (Wu and Luna 2001) introduced the numerical procedure for creep strain in mass concrete structure with temperature effects by modifying the exponential algorithm for concrete and the final formula for the incremental in strain (Eq. (13)) are presented below.

Let the total time travel [t_0, t] is subdivided into N steps, the creep strain increment column vector within step [t_{n-1}, t_n] may be generalized as

$$\left\{\Delta\varepsilon^c\right\} = [Q]\sum_{\gamma=1}^{3}\left[(1-e^{-S_\gamma\psi\tau_n\Delta\tau_n})\left\{\omega_{\gamma n}\right\} + \left\{\Delta\sigma_n\right\}\varphi_{\gamma n}h_{\lambda n}\right] = \left\{\eta_n\right\} + q_n[Q]\left\{\Delta\sigma_n\right\} \tag{13}$$

where

$$\left\{\eta_n\right\} = \sum_{\gamma=1}^{3}\left[(1-e^{-S_\gamma\psi\tau_n\Delta\tau_n})\left\{\omega_{\gamma n}\right\}\right] \tag{13a}$$

$$\left\{\omega_{\gamma n}\right\} = \left\{\omega_{\gamma n-1}\right\}e^{-S_\gamma\psi\tau_{n-1}\Delta\tau_{n-1}} + [Q]\left\{\Delta\sigma_{n-1}\right\}\varphi_{\gamma n-1}f_{\gamma n-1}e^{-Y_{n-1}} \tag{13b}$$

$$q_n = \sum_{\gamma=1}^{3}\varphi_{\gamma n}h_{\gamma n} \tag{13c}$$

$$h_{\gamma n} = 1 - f_{\gamma n}e^{-Y_n} \tag{13d}$$

$$Y_n = S_n\sum_{j=1}^{n}\psi_{Tj}\Delta_{Tj} \tag{13e}$$

$$f_{\gamma n} = \frac{1}{\Delta\tau_n}\int_{t_{n-1}}^{t_n}e^{y_S(\tau)} \tag{13f}$$

$$[Q]=\begin{bmatrix} 1 & -v & -v & 0 & 0 & 0 \\ & 1 & -v & 0 & 0 & 0 \\ & & 1 & 0 & 0 & 0 \\ & & & 2(1+v) & 0 & 0 \\ & Sym. & & & 2(1+v) & 0 \\ & & & & & 2(1+v) \end{bmatrix}, \; v \text{ is the Poisson's ratio} \tag{13g}$$

The corresponding stress increment can be obtained

$$\{\Delta\sigma_n\}=[D_n^{'}]\left(\{\Delta\varepsilon_n\}-\{\eta_n\}-\{\Delta\varepsilon_n^T\}\right) \tag{14}$$

$$[D_n^{'}]=\frac{[D_n]}{(1+q_nE_n)} \tag{14a}$$

where $[D_n]$ is the elastic matrix at the n^{th} time interval, which calculated based on the model in Eq. (7). Consequently, $[D_n]$ can be redefined as elastic matrix for RCC material which includes the aging and temperature effect. The full details of the mathematical derivation are given in the previous work of the authors (Abdulrazeg *et al*. 2010).

7. Safety evaluation against cracking

Two different formulation are used in the analysis of cracking in concrete structures are nonlinear fracture theory and continuum damage theory (Moyer *et al*. 1997). Due to the numerical drawbacks in the first theory the recent researchers have looked for the development of the later one (Bažant and Oh 1983).

In continuum damage mechanics (CDM) the stress strain relationships is used during the analysis and the cracking process will be initiated when the maximum value of the principle stress reaches the allowable tension stresses. The CDM approach is used in this study to propose a cracking criterion. In addition, the respective failure criteria for mass concrete in principal stress space and octahedron stress space which proposed by Wang and Song (2008) is adopted in research work.

The cracking criterion suggested by Wang and Song (2008) is a function of octahedral shear stress τ_{oct} and octahedral normal stress σ_{oct}

$$\sigma_{oct}=\frac{(\sigma_1+\sigma_2+\sigma_3)}{3} \tag{15}$$

$$\tau_{oct}=\frac{1}{3}\left[(\sigma_1-\sigma_2)^2+(\sigma_2-\sigma_3)^2+(\sigma_3-\sigma_1)^2\right]^{1/2} \tag{16}$$

Let σ_1, σ_2 and σ_3 denote the tensile stress, intermediate stress and compressive stress at failure under triaxial C-C-T, respectively, $f_t(t)$ the uniaxial tensile strength, and $f_c(t)$ the uniaxial compressive stress. The values of σ_{oct}/f_t and τ_{oct}/f_t will be regressed in a parabolic formula as follow (Wang and Song 2007)

$$\frac{\tau_{oct}}{fc} = 0.0655 - 0.9097\frac{\sigma_{oct}}{fc} - 0.08936\left(\frac{\sigma_{oct}}{fc}\right)^2 \tag{17}$$

This formula to be compatible with RCC construction sequence further modified as

$$\tau_{oct}(t)^{ult} = \left[0.0655 - 0.9097\frac{\sigma_{oct}(t)}{fc(t)} - 0.08936\left(\frac{\sigma_{oct}(t)}{fc(t)}\right)^2\right] f_c(t) \tag{18}$$

In triaxial tension, $\sigma_1 > \sigma_2 > \sigma_3 > 0$ the triaxial tensile strength is equal to uniaxial tensile strength $f_t(t)$. In tension - compression- compression (T-C-C), $\sigma_1 > 0$ and $\sigma_2 < \sigma_3 < 0$ the maximum strength is given by Eq. (18).
Taking into account this criterion, cracking on an element begins where the relation ψ_{cr} drop below the allowable value. The crack index

$$\psi_{cr} = \frac{\tau_{oct}(t)^{ult}}{\tau_{oct}(t)} \tag{19}$$

It can be verified that when $\psi_{cr} > 1.0$ the element is not cracked and cracking occurs when $\psi_{cr} < 1.0$.
The variation in the compressive strength with time is calculated according to ACI, which relates the elastic modulus to the compressive strength as

$$E(t) = 4750\sqrt{f_c(t)} \tag{20}$$

where $E(t)$ is the elastic modulus, which is time and temperature dependent Eq. (7).
The tensile strength of RCC material is evaluated using the model that developed by Zdiri *et al*. (2008) and described by Eq. (21).

$$f_t = 0.214 f_c^{0.69} \tag{21}$$

Finally, the allowable octahedral shear stress will be determined using Eq. (18) based on that the crack safety factor is generated by Eq. (19).
If safety coefficient of crack is greater than one, the element will be considered safe against crack. But if the coefficient is less than one, crack will develop in the dam body.

8. Computational algorithm of creep and temperature effect

The computational procedures followed in this study to account for creep and temperature effects are summarized as follows:
i) Using procedure in the section 2 the temperature field $T(t)$ is computed.
ii) Substituting T into Eqs. (8), (9), $\beta(t)$ and $\psi(t)$ will be evaluated.
iii) Determine the equivalent age and elastic modulus for the n^{th} interval time.
iv) Calculate the constants of Eq. (13)
v) Determine q_n, η_n

vi) Calculate the transient thermal creep using Eq. (11)
vii) Calculate the equivalent nodal loads include temperature, creep, transient creep and external.
viii) Determine displacement increment, and based on that calculate the column matrix of stress increment at n^{th} time interval.
ix) Calculate the total stress at n^{th} time.
x) Repeat step (i) to (vii) until the construction of the stage is completed.
Fig. 1 illustrates the code flow chart based on the above computational steps.

9. Development of finite element code

In previous discussion, formulation in Sections (3, 4 and 5) for temperature, creep and crack analysis are implemented into ongoing research program (Abdularzeg 2011). Based on that, a three- dimensional finite element program was developed and the following are the features of the finite element code:
i. Thermal analysis
ii. Structural analysis with or without creep effect
iii. Combined thermal and structural analysis with or without creep effect
iv. Crack safety evaluation
The developed finite element program is written in FORTRAN language and can work under power station environment. The flowchart shown in Fig. 2 represents the architecture of the program. The main program calls 26 main subroutines, each main subroutine calls another sub-subroutines and the code is about 6112 lines. The general procedures followed in the stress analysis are presented in Fig. 2 (Abdularzeg 2011).

10. Verification of the proposed model

In order to validate the proposed mathematical modeling, computational algorithm and the developed finite element program, a concrete block which was reported in the literature by Wu and Luna (2001) has been analyzed. The block geometry is shown in Fig. 3. The material properties are summarized in Table 1. The upper surface of the block is exposed to the air and the ambient temperature is 10°C. The creep constants for concrete material are tabulated in Table 2.

Fig. 4(a) shows the temperature at the central point of the concrete block. The temperature increases due to the heat produced by hydration, then reaches a maximum point at about 8 days

Table 1 Thermal and structural properties of concrete block (Wu and Luna 2001)

Material	Concrete
Heat conduction coeff. K (W/m °C)	2.16
Heat convection coeff. h (W/m^2 °C)	8.0
Specific heat c (J/kg °C)	1150
Density ρ (kg/ m^3)	2400
Elasticity modulus E (kg/ m^2)	2.6×10^9
Poisson ratio ν	0.16

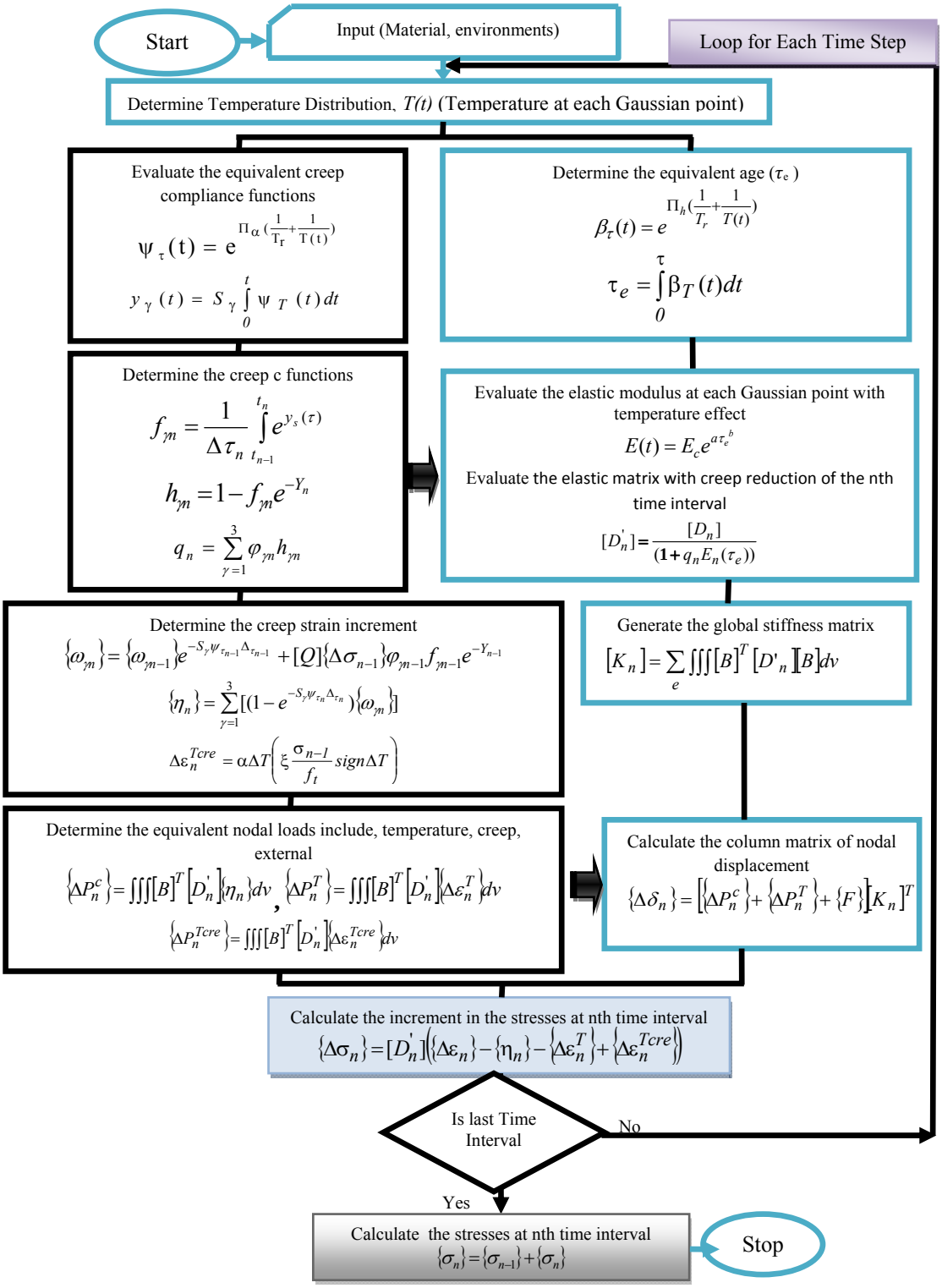

Fig. 1 Flow chart for computational procedures of creep and temperature effect

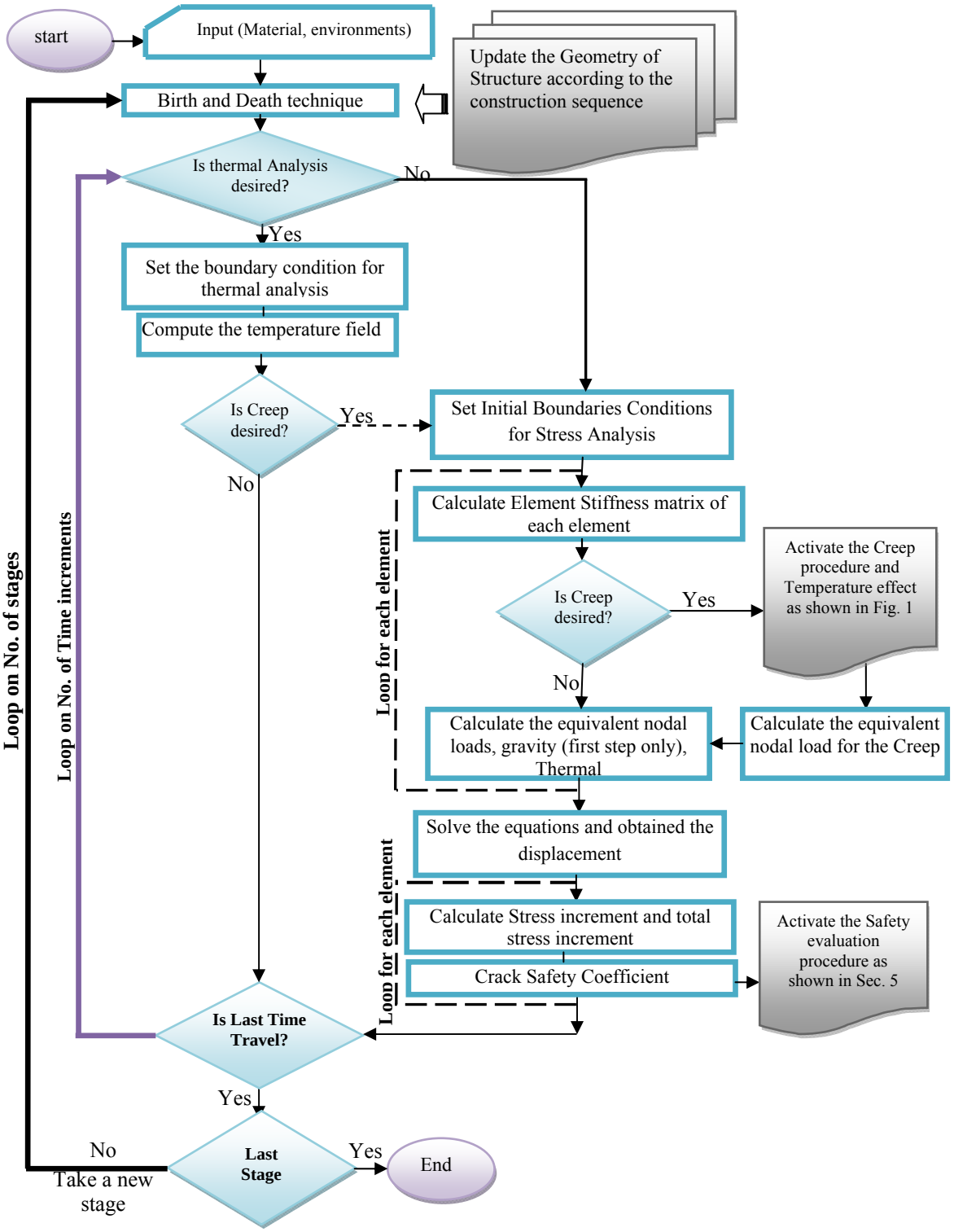

Fig. 2 Program flow chart (with temperature and creep modification)

Table 2 Creep Constants (Wu and Luna 2001)

	α_i	β_i	δ_i	D
1	0.35494	0.48368	0.35361	…..
2	3.73350	-0.18600	0.01248	…..
3	-2.56440	0.13786	0.03264	0.83509

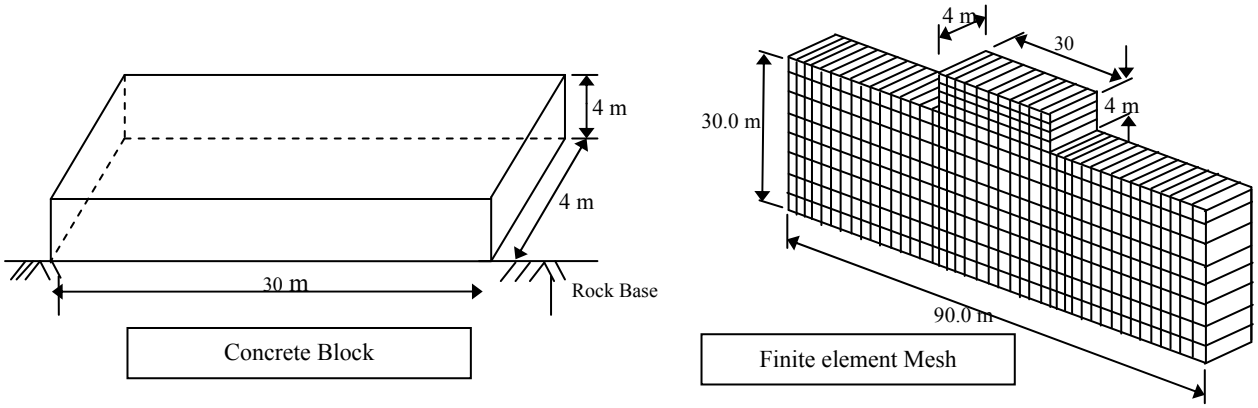

Fig. 3 Concrete block

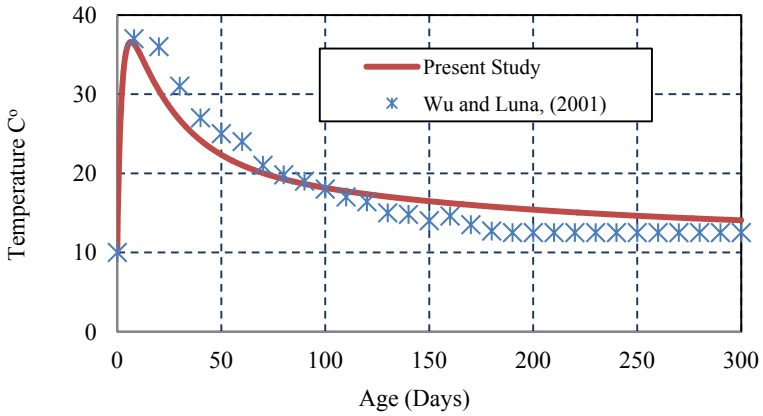

Fig. 4(a) Temperature variation at the central point

after casting. Then the block starts to cool down due to the interaction with ambient temperature. Fig. 4(b) shows the variation of the thermal stress along the same point of the block. The maximum compression stress also occurs at about 8 days after the block is cast. Then the compression stress decreases which is expected because the block begins to cool down. Finally, the compression stress changes to tension stress and the tension stress becomes larger and larger because the block continues to cool down.

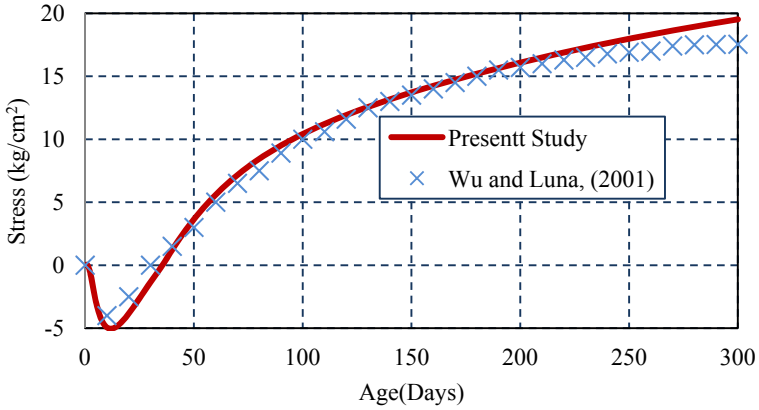

Fig. 4(b) Stress variation at the central point of the block

Table 3 Creep data for RCC and CVC materials (Zhang 1995)

Material		α_i	β_i	δ_i	D
CVC	1	0.35494	0.48368	0.35361	……..
	2	3.7335	-0.186	0.012486	……..
	3	-2.5644	0.13786	0.032642	0.83509
RCC	1	0.058864	0.38362	1.356	…….
	2	7.4729	-11.115	0.08919	…….
	3	-5.2079	7.9619	0.078675	4.2808

11. Analysis of actual RCC dam

11.1 Description of Kinta dam

A brief description of the Kinta RCC dam project is given in previous work of authors (Noorzaei *et al*. 2009). The reader may refer to it for details about the progress of the dam construction with respect to time and the geometry of the dam as well as the material properties of the different types of concrete used in the foundation, body, and faces. The creep experimental data which reported in the literature by Zhang (1995) for RCC and CVC materials has been adopted in present study, these data tabulated in the Table 3.

11.2 Initial conditions

The temperature distribution in the rock foundation and the RCC placing temperature are the two initial conditions considered in the analysis.

11.2.1 Evaluation of the foundation temperature

The determination of the foundation initial temperature is usually performed by the thermal analysis of the block foundation for a period of two or three years prior to the dam construction time (Ishakawa 1991). However, since the Kinta dam is located in a tropical area where the average monthly temperature is the almost same throughout the year, the average annual

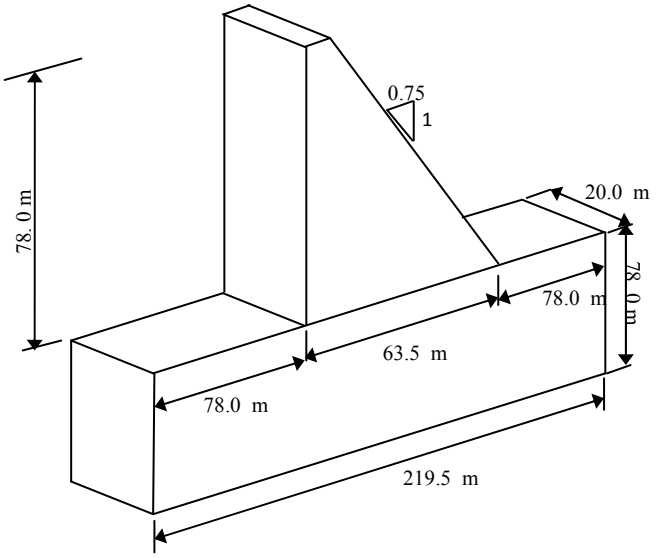

Fig. 5 Geometry of Kinta dam

temperature at the project site (28 ºC) has been assigned to the nodes of the block foundation as an initial condition.

11.2.2 RCC placing temperature

For the Kinta RCC dam, the RCC placing temperature is maintained below 30˚C as the upper limit of the placing temperature taken in the design of the dam. Hence, for the performed thermal analysis in this research, the RCC placing temperature is taken as 30˚C for all laid RCC lifts.

11.3 Finite element modeling

Two finite element models have been prepared in the present study.

(a) Finite Element Model without Reservoir (Dam body/Foundation)

The 3D finite element model of the deepest block is shown in Fig. 6(a). Twenty node isoparametric element is used for the propose discretization of dam body, foundation and reservoir. The finite element of the dam body is generated in such a way to present the construction phase.

(b) Finite Element Model with Reservoir.

The finite element model used to simulate the heat exchange between the impounding water and dam body at the upstream side is shown in Fig. 6(b) .The elements which model the water are assumed to be added in layers according to the reservoir filling schedule. The thickness of each water layer is kept equal to the corresponding opposite RCC lift in order to maintain the finite element continuities.

12. Result and discussion

12.1 Temperature distribution during the construction

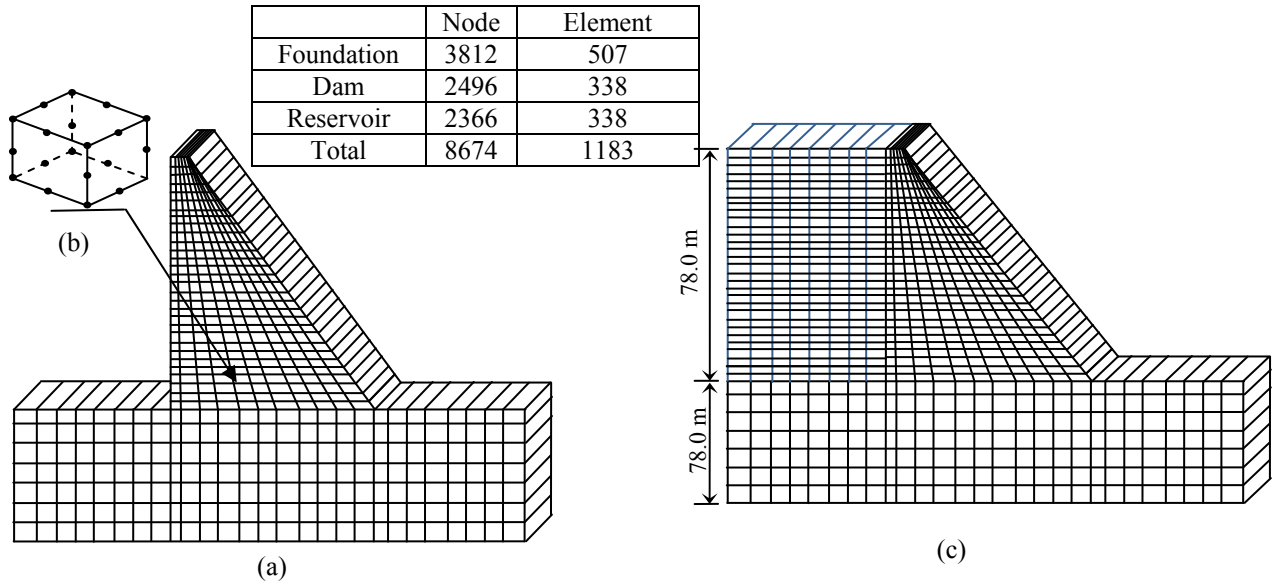

	Node	Element
Foundation	3812	507
Dam	2496	338
Reservoir	2366	338
Total	8674	1183

Fig. 6 Three- dimensional Finite Element Model- Mesh (a)Dam foundation system (b) Twenty node isoparametric element (c) Dam body, foundation block, and reservoir system

The plots of temperature distribution in the body of the dam for the different constructed lifts are shown in Fig. 7. It is seen form this plot that, the maximum temperature predicted is 43°C, it was formed at the bottom of the dam during the construction. This can be due to the use of higher RCC placement temperatures combined with higher insulating property of this region due its massive volume compared with the other locations. The maximum temperature predicted after the end of construction was 41°C in the core of the dam which gradually decreased to reach approximately the air temperature at the boundaries.

The variation of temperature with time for the center point of the dam at an elevation of 13.5 m form the base is depicted in Fig. 8. The plot demonstrates that, the maximum temperature in the dam body on 18 October was about 43°C which 10 days after the casting of the lift. This rise is attributed to the hydration of the cement at early age. Then the temperature starts to cool down to reach 40°C and remains nearly constant during the construction.

12.2 Temperature distribution during reservoir filling

An attempt has been made to draw the water interaction isothermal profiles for a different level of the reservoir pounding and the similar plots for one and three years as shown in Fig. 9. The idealization of the reservoir mesh is set using the methodology given by Bayagoob *et al*. (2010). The maximum predicted temperature at the dam body center is 41°C (at end of construction) after the reservoir is filled the temperature dropped to 40°C as shown in Fig. 9. After one year it dropped to 39°C and to 37°C after 3rd years. The heat dissipation at the downstream side is higher than that at the upstream side, this may be due to the high insulating property of the dam reservoir resulting from its huge volume combined by the low conductivity of water.

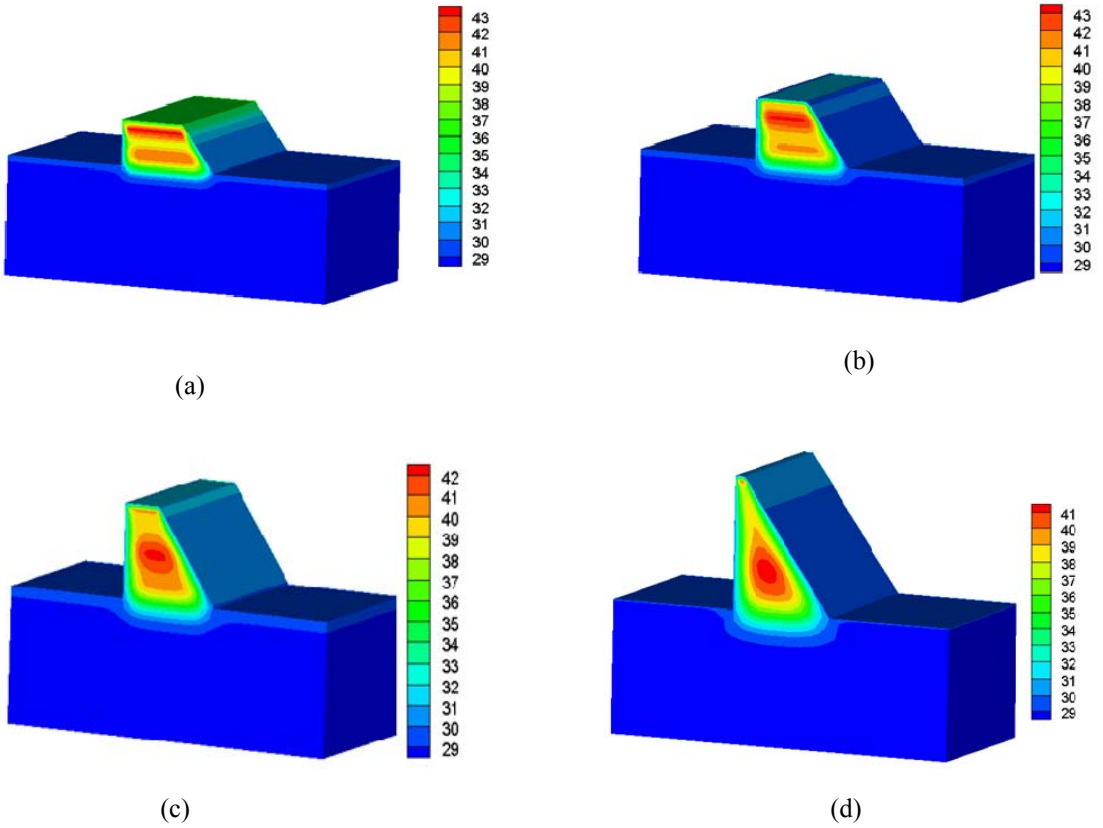

Fig. 7 Temperature distribution for different lifts: (a) temperature distribution at Lift 10; (b) temperature distribution at Lift 13; (c) temperature distribution at Lift 21; (d) temperature distribution at the end of construction

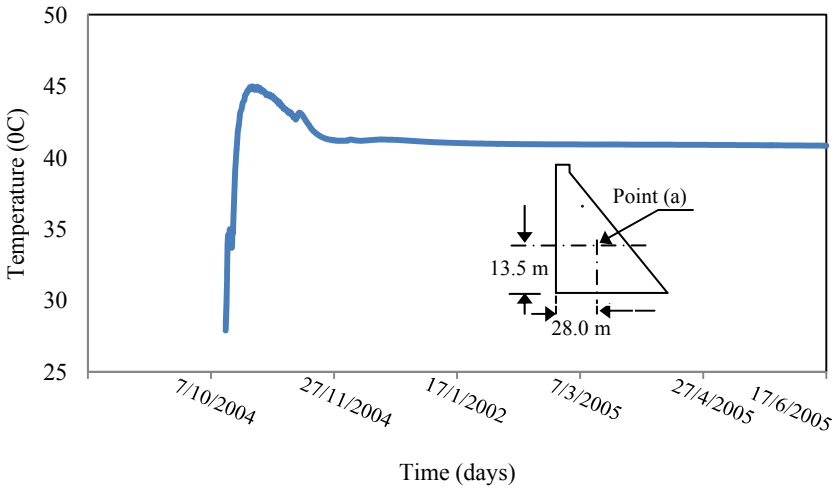

Fig. 8 Predicted temperature history at 13.5 m from the base measured at the center of the dam

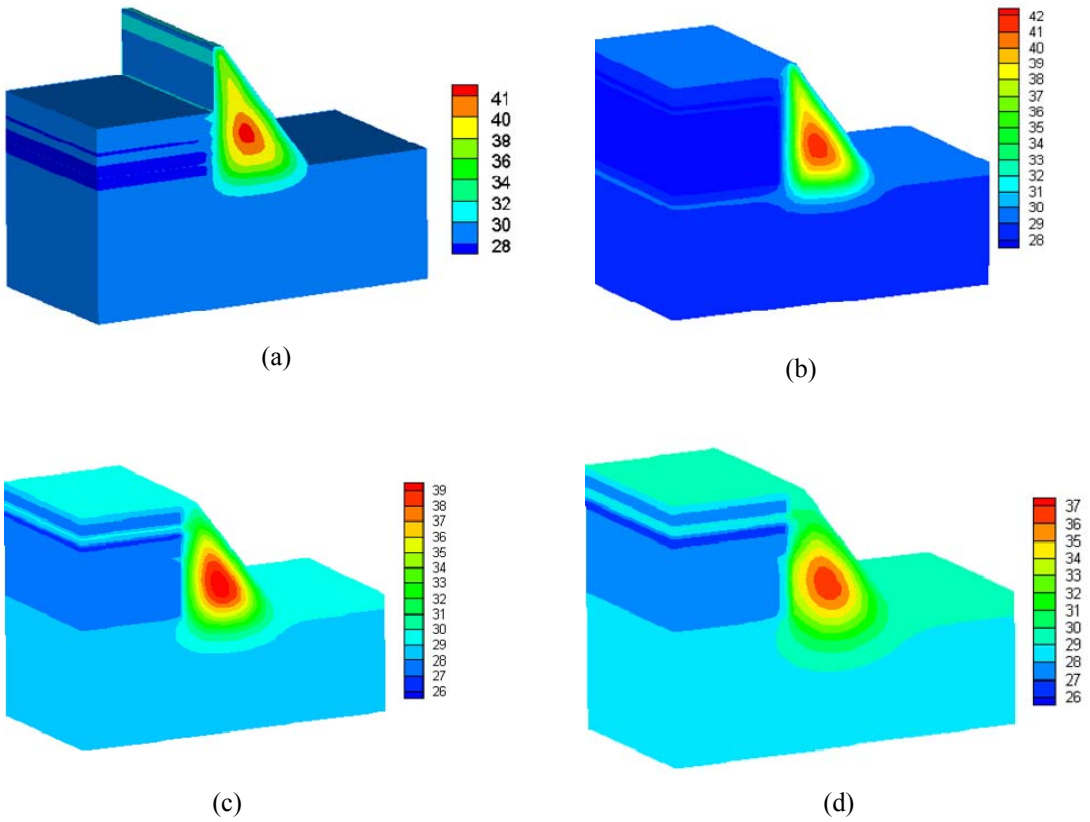

Fig. 9 Water- dam body interaction thermal response:(a) One year; (b) Two years ;(c) Three years

12.3 Temperature effect on the elastic modulus

In order to investigate the effect of the temperature on the variation of the elastic modulus, Fig. 10 presents the temperature at the particular point (a). It is obvious from the plot there is a significant difference between the two curves of the elastic modulus during the initial stage due to the high temperature of hydration. If the temperature effect was considered, the elastic modulus is increased by 45% at the first 10 days. However, the ultimate elastic modulus is not significantly effect.

12.4 Stress simulation

In this section, the results from stress analysis preformed on a numerical model of Kinta RCC dam subjected to combined loading of thermal, gravity, creep and hydrostatic load are presented. Results from the reference case study, simulating the real construction process and the first 3 years of the RCC dam's service life are discussed. This will provide the assessment of the dam design and the actual short- and long-term safety conditions of the construction and service life.

Fig. 11 represents the principal stresses at the center of the dam for different heights of the

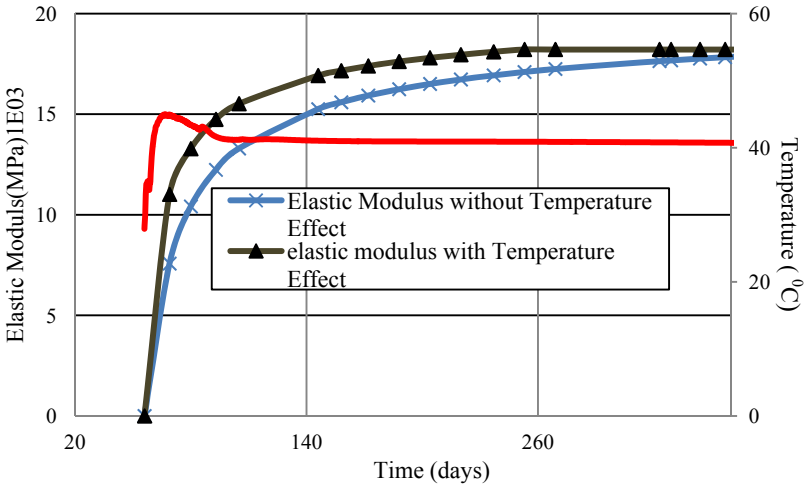

Fig. 10 Temperature and the variation of the elastic modulus at the central point

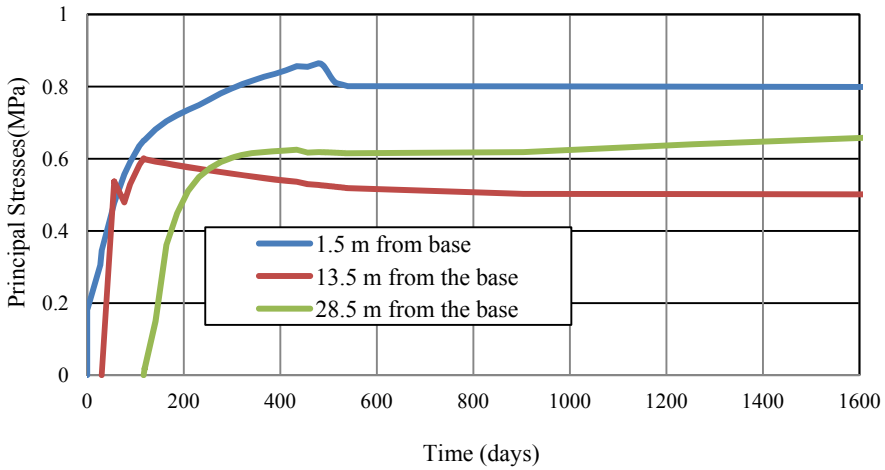

Fig. 11 Principal stresses at center of dam

dam. The results indicated that the first peak tensile stress occurs shortly after placement of the RCC layers within first 10 days after the casting of the left. The tensile stress then increases and remains almost constant during construction before the reduction because of the effect of the reservoir load on the upstream face.

Fig. 12 shows Principal stresses history at 13.5 m from the base measured at the center of the dam. The result indicated that, the stress has been increased. When the temperature effects are considered, the maximum principle stresses increased from 0.43 MPa to 0.61 MPa by 41% in the initial stage. This is attributed to high temperature rising from the hydration at the initial stage is. However, in the long term stress the stresses will be reduced and this may attributed to the creep effect.

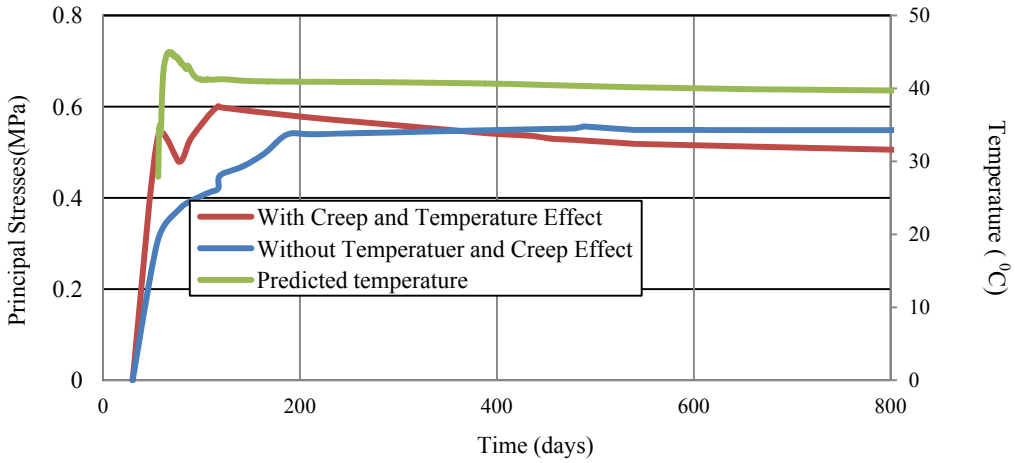

Fig. 12 Principal stresses history at 13.5 m from the base measured at the center of the dam

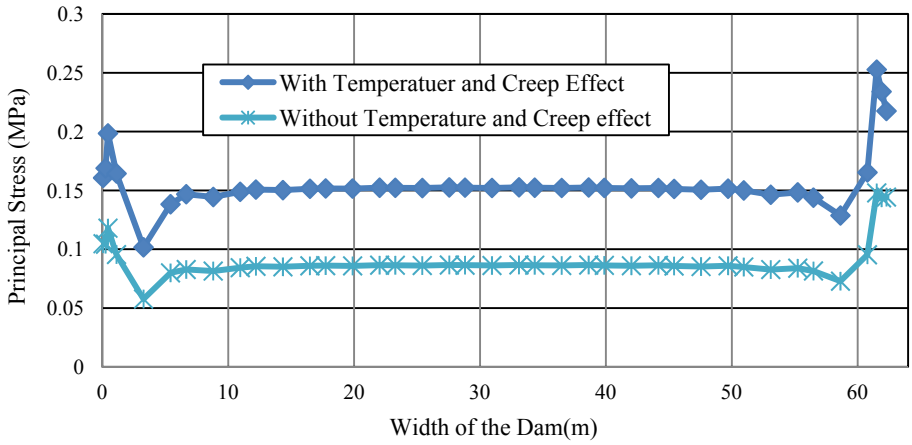

Fig. 13(a) The principal stress path along the dam width after the casting

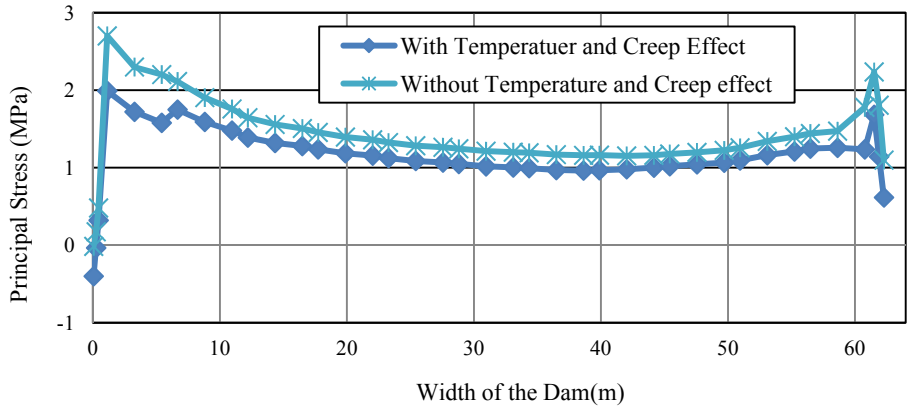

Fig. 13(b) The principal stress path along the dam width after three year

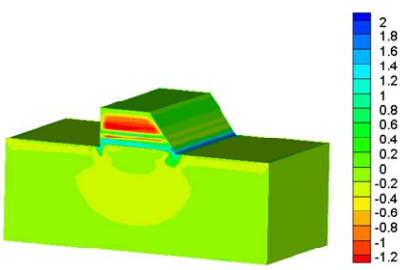

(a) Maximum principal stress distribution at Lift 10

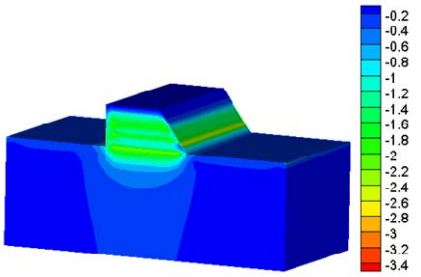

(b) Minimum principal stress distribution at Lift 10

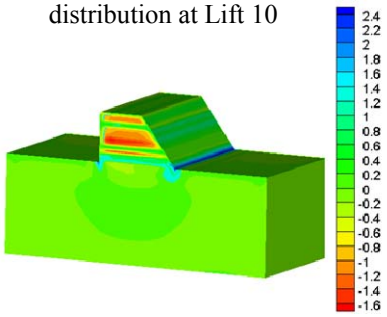

(c) Maximum principal stress distribution at Lift 13

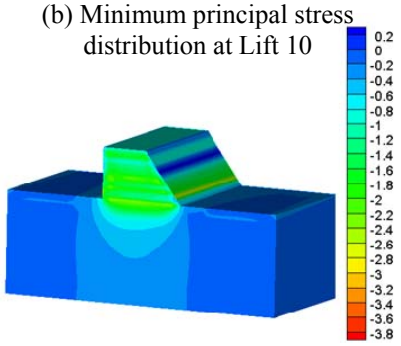

(d) Minimum principal stress distribution at Lift 13

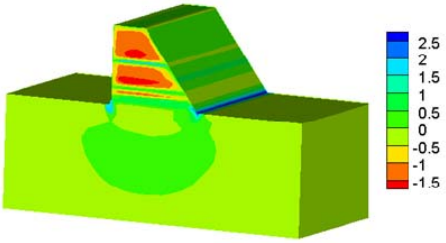

(e) Maximum principal stress distribution at Lift 21

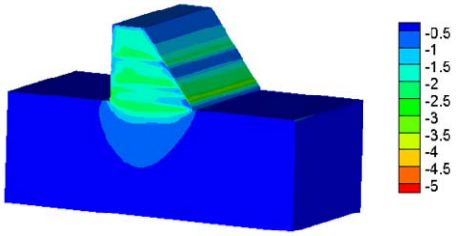

(f) Minimum principal stress distribution at Lift 21

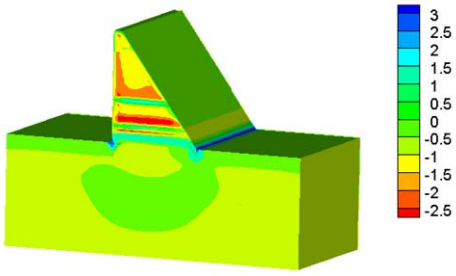

(g) Maximum principal stress distribution at the end of construction

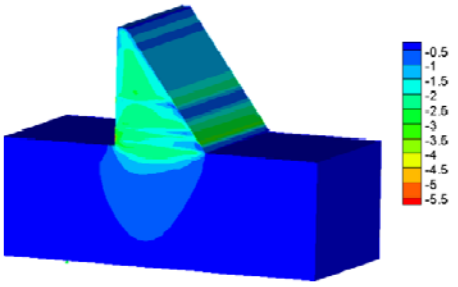

(h) Minimum principal stress distribution at the end of construction

Fig. 14 Three-dimensional principal stress distribution in body of the dam

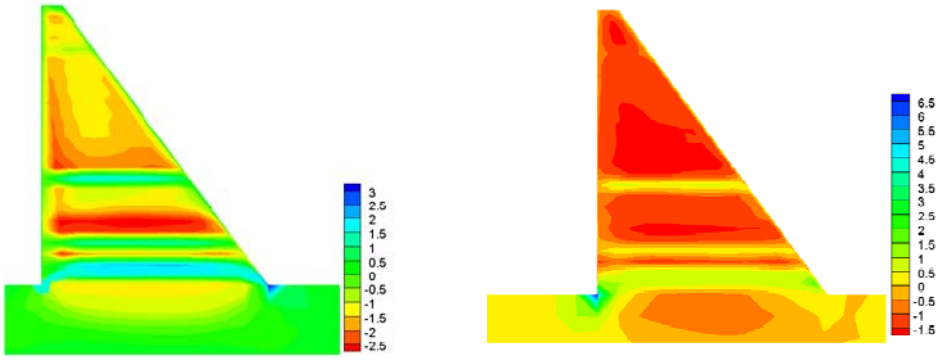

(a) (b)

Fig. 15 principal stress distribution in body of the dam : (a) maximum principal stress distribution at the end of construction; (b) maximum principal stress distribution after the filling of the reservoir

Similar response has shown by Fig. 13(a), which shown the principal stress path along the dam width after completion of second stage within age of 6 days. It's clear that, the there is remarkably increase in the stresses due to the high temperature. When the temperature effects are considered, the maximum principle stresses increased from 0.087 MPa to 0.132 MPa by 49% in the initial stage. However, on the long term there is reduction in the principal stress as shown in Fig. 13(b).

Fig. 14 shows the principle stress contours developed in the dam body for different constructed lifts. The result indicate that, the tensile stress developed at different levels with the dam body during construction, the presence of high tensile stresses at the dam bottom with maximum value at the heel and increasing with constriction sequence to reach 3 MPa at the end of construction. Generally, it is observed that most of the dam body under compressive stresses.

Fig. 15 shows the comparison between the principal stresses at the end of construction and after the filling of the reservoir. The plot indicated that, the maximum tensile stress observed at the downstream side especially in the hell. This tensile are suppressed after filling of the reservoir. In addition, there is increase in the compressive stress at the downstream side after the filling of reservoir.

12.5 Cracking criteria and safety evaluation

Simultaneously during the stress analysis the crack safety factor will be calculated based on the Eq. (19) for each Gaussian point. Hence, all the properties of the materials are time and temperature dependent, especially elastic and strength properties, the variation of the crack factor with time and temperature are determined. Thus, this factor will be more realistic to represent the crack occurrence.

Fig. 16 shows the variation of crack index during the construction and operation of the dam. The corresponding elevation is 1.5 m from the base. It is clear from the plot that the dam is safe against cracking at upstream side during the construction stage. However, during the operation phase the crack index is dropped below the allowable limit and this attributed to the effect of the reservoir load at the upstream face. Contrary response at the downstream, where the crack index is bellow the allowable limit, and during the operation is within the limit. It can conclude that, the

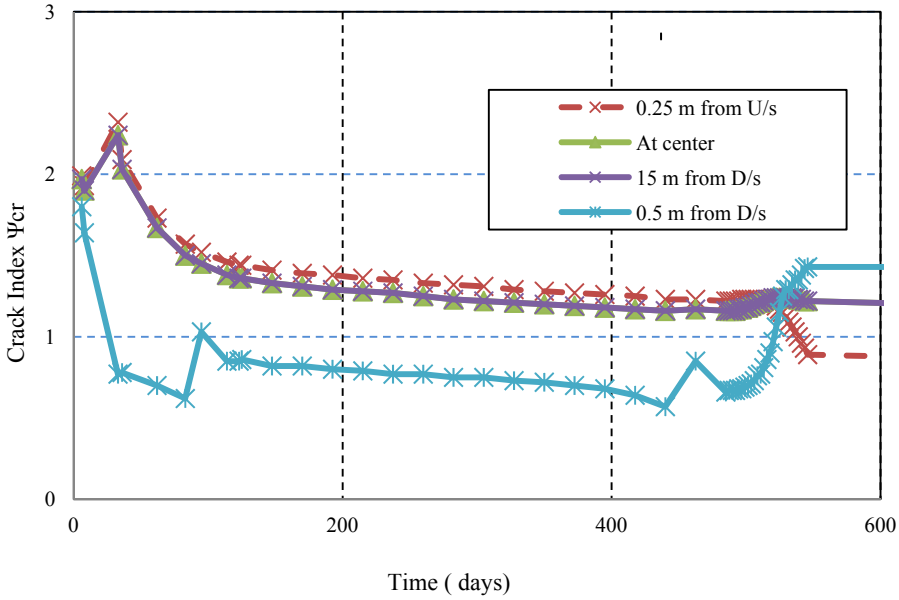

Fig. 16 Variation of the crack index

upstream and the downstream regions at this level (toe and hill) are the most probable crack regions where the crack index values are dropped below the limit value.

13. Conclusions

This paper introduces a methodology to analyze the unsteady temperature and stress fields of roller compacted concrete (RCC) dams. A viscoelastic model, which includes the ageing and temperature effect, was proposed for the RCC material. The methodology is presented as a numerical implementation using the finite element method for the simulation of the construction process and the first 3 years of service life of RCC dams. Safety against cracking is determined using a criterion which is dependent on the behavior of dam concrete under multi-axial stress states. A three-dimensional program was developed and a numerical example is used for verification of the methodology and program.

• A viscoelastic model, which includes ageing and temperature effects on properties of RCC materials, was developed. This model is able to predict the evolution in time of the thermally induced tensile stresses that develop during the construction and the service life; this allows one to assess the risk of occurrence of crack either at short or long term.

• The Conrad's model which expresses the variation of the elastic modulus of RCC material with time has been further modified to account for temperature effect.

• The result has shown that, If the temperature effects are considered, the maximum principle stresses increased by 40% in the initial stage. This is because the temperature at the initial stage is high due to hydration the elastic modulus is high also which increased the stress during this stage.

• For changing temperature, the transient creep is taken into account by an additional creep

term. The term depends on the state of stress and strength of concrete.

• Creep is normally beneficial in reducing stresses, but it might also lead to increased stresses. Under realistic temperature histories it might have negative effect on the cracking risk; because creep reduces compressive stresses, but increases the subsequent tensile stresses.

• The crack index variation can give a good indication of the probability of cracking with time.

• The tensile stress which developed at the downstream and upstream, will lead to drop in the crack safety factor in this zone, it can be concluded that special attention should be paid to this sides in design.

Acknowledgements

The writers thank the owner of Kinta dam, Lembaga Air Perak and Angkasa-GHD SDN Bhd in Malaysia for providing the data used in this paper.

References

Abdularzeg, A.A. (2011), "Modeling of combined thermal and mechanical actions in roller compacted concrete dam by finite element method", Ph.D. Thesis, Civil Engineering Department, Universiti Putra, Malaysia.

Abdulrazeg, A.A., Noorzaei, J., Khanehzaei, P., Jaafar, M.S. and Mohammed, T.A. (2010), "Effect of temperature and creep on roller compacted concrete dam during the construction stages", *Computer Modeling in Engineering & Sciences*, **68**(3), 239-268.

Agullo, L. and Aguado, A. (1995), "Thermal behavior of concrete dams due to environmental actions", *Dam Eng*., **VI**(1), 3-21.

Atrushi, D.S. (2003), "Tensile and compressive creep of early age concrete: testing and modeling", Ph.D. Thesis, Department of Civil Engineering, Norwegian University of Science and Technology, Norwegian.

Bayagoob, K.H., Noorzaei, J., Abdularzeg, A.A., Al-Karni, A.A. and Jaafar, M.S. (2010), "Coupled thermal and structural analysis of roller compacted concrete arch dam by three-dimensional finite element method", *Structural Engineering and Mechanics*, **36**(4), 401-419.

Bayagoob, K.H., Noorzaei, J., Jaafar, M.S., Thanoon, W.A. and Abdulrazeg, A.A. (2010), "Modelling heat exchange between RCC dam and reservoir", *Proceedings of the ICE-Engineering and Computational Mechanics*, **163**(1), 33-42.

Bazant, Z.P., Cusatis, G, and Cedolin, L. (2004), "Temperature effect on concrete creep modeled by microprestress-solidification theory", *Journal of Engineering Mechanics-Proceedings of the ASCE*, **130**(6), 691-699.

Bazant, Z.P. and Oh, B. (1983), "Crack band theory for fracture of concrete", *Materials and Structures*, **16**(3), 155-177.

Bombich, A.A. (1987), Thermal Stress Analyses of Mississippi River Lock and Dam 26 (R), Vicksburg, Miss., Army Engineer Waterways Experiment Station Vicksburg MS Structures Lab.

Bosnjak, D. (2000), "Self-induced cracking problems in hardening concrete structures", Ph.D. Thesis, Civil Eng. Dept., Norwegian University of Science and Technology, Norwegian.

Cervera, M., Oliver, J. and Prato, T. (2000a), "Simulation of construction of RCC dams. I: temperature and aging", *Journal of Structural Engineering*, **126**, 1053.

Cervera, M., Oliver, J. and Prato, T. (2000b), "Simulation of construction of RCC dams. II: Stress and damage", *Journal of Structural Engineering*, **126**, 1062.

Conrad, M., Aufleger, M. and Malkawi, A. (2003), Investigations on the modulus of elasticity of young RCC", *Proceedings of the fourth international symposium on roller compacted concrete (RCC) dams*,

Madrid, Spain.
Crichton, A., Benzenati, I., Qiu, T. and Williams, J. (1999), "Kinta RCC dam-are over-simplified thermal structural analysis", ANCOLD Issue (115).
deAraujo, J. M. and Awruch, A.M. (1998), "Cracking safety evaluation on gravity concrete dams during the construction phase", *Computers & Structures*, **66**(1), 93-104.
Du, C. and Liu, G. (1994), "Numerical procedure for thermal creep stress in mass concrete structures", *Communications in Numerical Methods in Engineering*, **10**(7), 545-554.
Fehl, B.D., Normal, C.D. and Truman, K.Z. (1988), "Parameters affecting stresses in mass concrete structures", *Proceedings of the Corps of Engineers Structural Engineering Conference*, St. Louis, MO.
Hedlund, H. (1996), "Stresses in high performance concrete due to temperature and moisture variations at early ages", Ph.D. Thesis, Division of Structural Engineering, Sweden.
Ishikawa, M. (1991), "Thermal stress analysis of a concrete dam", *Computers & Structures*, **40**(2), 347-352.
Jaafar, M.S., Bayagoob, K.H., Noorzaei, J, and Thanoon, W.A.M. (2007), "Development of finite element computer code for thermal analysis of roller compacted concrete dams", *Advances in Engineering Software*, **38**(11-12), 886-895.
Jonasson, J.E. (1994), "Modelling of temperature, moisture and stresses in young concrete", Ph.D. Thesis, Structural engineering, Lulea University of Technology, Sweden.
Lingfei, X. and Li, Y. (2008), "Research on temperature control and anti-cracking simulation for xiaowan concrete high arch dam", *Water Power*, 1036-1039.
Luna, R. and Wu, Y. (2000), "Simulation of temperature and stress fields during RCC dam construction", *Journal of Construction Engineering and Management*, **126**(5), 381-388.
Malkawi, A.I.H., Mutasher, S.A. and Qiu, T.J. (2003), "Thermal-structural modeling and temperature control of roller compacted concrete gravity dam", *Journal of Performance of Constructed Facilities*, **17**, 177.
Moyer, E.T., McCoy, H. and Sarkani, S. (1997), "Prediction of stable crack growth using continuum damage mechanics", *International Journal of Fracture*, **86**(4), 375-384.
Neville, A.M., Dilger, W.H. and Brooks, J.J. (1983), *Creep of plain and structural concrete*, Construction Press London.
Noorzaei, J., Bayagoob, K., Abdulrazeg, A., Jaafar, M. and Mohammed, T. (2009), "Three dimensional nonlinear temperature and structural analysis of roller compacted concrete dam", *Computer Modeling in Engineering & Sciences*, **47**(1), 43-60.
Noorzaei, J., Bayagoob, K.H., Thanoon, W.A. and Jaafar, M.S. (2006), "Thermal and stress analysis of Kinta RCC dam", *Engineering Structures*, **28**(13), 1795-1802.
Saetta, A., Scotta, R. and Vitaliani, R. (1995), "Stress analysis of concrete structures subjected to variable thermal loads", *Journal of Structural Engineering*, **121**(3), 446-457.
Santurjian, O. and Kolarow, L. (1996), "A spatial FEM model of thermal stress state of concrete blocks with creep consideration", *Computers & Structures*, **58**(3), 563-574.
Sheibany, F. and Ghaemian, M. (2006), "Effects of environmental action on thermal stress analysis of karaj concrete arch dam", *Journal of Engineering Mechanics*, **132**, 532.
Thelandersson, S. (1987), "Modeling of combined thermal and mechanical action in concrete", *Journal of Engineering Mechanics*, **113**, 893.
Truman, K.Z. (1991), "Creep, shrinkage, and thermal effects on mass concrete structure", *Journal of Engineering Mechanics*, **117**(6), 1274-1288.
Wang, H. and Song, Y. (2008), "Behavior of dam concrete under biaxial compression-tension and triaxial compression-compression-tension stresses", *Frontiers of Architecture and Civil Engineering in China*, **2**(4), 323-328.
Wu, Y. and Luna, R. (2001), "Numerical implementation of temperature and creep in mass concrete", *Finite Elements in Analysis and Design*, **37**(2), 97-106.
Yuan, Y. and Wan, Z. (2002), "Prediction of cracking within early-age concrete due to thermal, drying and creep behavior", *Cement and Concrete Research*, **32**(7), 1053-1059.
Zdiri, M., Ouezdou, M.B. and Neji, J. (2008), "Theoretical and experimental study of roller-compacted

concrete strength", *Magazine of Concrete Research*, **60**(7), 469-474.
Zhang, M.L. (1995), "Study on structural treatment, stress and stability of roller compacted concrete gravity dam", Department of Hydraulic and Hydropower Engineering, Tsinghua University, Beijing, China.
Zhang, X., Li, S., Chen, Y. and Chai, J. (2009), "The development and verification of relocating mesh method for the computation of temperature field of RCC dam", *Advances in Engineering Software*, **40**(11), 1119-1123.